WPPFC-CPR(18) 20655

R Dejarnac et al.

Physics of toroidal gap heat loading on castellated plasma-facing components

Preprint of Paper to be submitted for publication in Proceeding of 23rd International Conference on Plasma Surface Interactions in Controlled Fusion Devices (PSI-23)

This work has been carried out within the framework of the EUROfusion Consortium and has received funding from the Euratom research and training programme 2014-2018 under grant agreement No 633053. The views and opinions expressed herein do not necessarily reflect those of the European Commission.

Physics of toroidal gap heat loading on castellated plasma-facing components

R. Dejarnac[a,*], J. P. Gunn[b], P. Vondracek[a,c], M. Komm[a], R. A. Pitts[d]

[a]*Institute of Plasma Physics, Czech Academy of Sciences, 182 00 Prague, Czech Republic*
[b]*CEA, IRFM, F-13108 Saint-Paul-lez-Durance, France*
[c]*Faculty of Mathematics and Physics, Charles University, 121 16 Prague, Czech Republic*
[d]*ITER Organisation, Route de Vinon-sur-Verdon, CS 90 046, F-13067 St Paul-lez-Durance cedex, France*

[*]*corresponding author: Renaud Dejarnac dejarnac@ipp.cas.cz*

Abstract

Because the gaps between plasma-facing components in fusion devices are comparable in size to the ion Larmor radius (of the order of 1 mm), magnetic field line tracing, the so-called "optical approximation", cannot accurately predict the fine scale heat load distribution around the gap edges. Finite Larmor radius effects dominate ion deposition. The poloidal component of the ion flux striking the surface is always in the diamagnetic drift direction, meaning that ions preferentially load one side of the gap. Usually electrons can be described optically due to their smaller Larmor radius. Depending on the local inclination of magnetic flux surfaces, it is possible that ions and electrons wet the same side of the gap, or opposite sides. Two-dimensional particle-in-cell simulations and dedicated experiments performed in the COMPASS tokamak are used to better understand processes responsible for plasma deposition on the sides of toroidal gaps between castellated plasma-facing components in tokamaks. The different contributions of the total incoming flux along a toroidal gap have been observed experimentally for the first time in COMPASS. These experimental results confirm the model predictions, demonstrating that in specific cases the heat deposition does not necessarily follow the optical approximation. The role played by electric fields in the deposition pattern is marginal, on the contrary to local non-ambipolarity that can change the asymmetrical plasma deposition from one side of the toroidal gap to the other.

1. Introduction

For power handling reasons, the water cooled, plasma-facing components in the ITER tungsten divertor will be castellated, comprising tens of thousands of individual monoblocks (MB) [1]. Gaps in both the toroidal (TG) and poloidal (PG) directions introduce leading edges onto which plasma heat flux can be focused, even if misalignments between neighboring MBs are eliminated. Decomposing the total particle/heat flux flowing into TGs as the sum of the ion and electron contributions and accounting for their 3D trajectories, the theory says that, depending on the magnetic configuration, regions which would be shadowed in a purely optical picture can be accessed by ions with finite Larmor radius, a problem which can be particularly acute during Edge Localized Modes (ELM) when energetic ions from the pedestal region impact the target during the transient heat pulse. Heat loads on the ITER MBs were recently assessed using 3D ion orbit calculations [2,3], guiding efforts to find a shaping solution which avoids gap edge over-heating. If toroidal beveling will hide leading edges on each side of PGs from inter-ELM heat loads (at the expense of higher perpendicular loads on the top surface), no solution for hiding all the long TG edges on both inner and outer ITER vertical targets has yet been found. The ion orbit simulations predict that even mitigated ELMs can melt TG edges in the strike point regions, posing a potential risk to MB lifetime.

Although the consequences of TG loading may be significant for ITER, the phenomenon had never actually been seen in a tokamak until a series of dedicated experiments, reported here, was performed on the COMPASS tokamak. The low magnetic field in COMPASS makes the ratio of the ion Larmor radius to the gap width relevant to ITER ELMing conditions. Using special instrumented central column graphite tiles bearing TGs, viewed with a high spatial resolution (0.5 mm/pixel) infra-red camera diagnostic, clear evidence for TG heating has been obtained for the first time. By changing the direction of the poloidal and toroidal magnetic fields, the four possible configurations of field line interactions with TGs have been examined. The experimental surface temperature profiles, proportional to heat load distributions, have been compared qualitatively with heat flux profiles derived from both the optical approximation (OA) and simulations using the 2D particle-in-cell (PIC) code SPICE2D [4], including self-consistent electric fields.
In two of the field configurations, plasma flux is observed to impinge on the unshadowed TG side only, as expected optically and as expected at the ITER outer vertical target (OVT), but in the other two, heat is deposited on both gap sides, and therefore in the magnetically shadowed regions as expected at the ITER inner vertical target (IVT), in excellent agreement with the theory and the SPICE2D code results. This same code has been used to benchmark the 3D ion orbit calculations for ITER [5], providing confidence both in the existence of the TG loading phenomenon and in the validity of the simpler ion orbit approach. It is known that the electric field plays a role in the plasma deposition around leading edges and PG [4]. Here, the effect of electric fields is assessed by comparing PIC simulations with ballistic simulations using the same code but forcing the electric field to zero. The comparison experiment vs. code has also emphasized the role played by local non-ambipolarity in determining the distribution of heat loading. In a separate experiment, time-varying bias voltage waveforms have been applied to a specially designed electrically insulated TG to select between electron-dominated and ion-dominated regimes. In the case of the two-sided deposition and depending on the bias voltage, the heat load is observed to switch sides, following theoretical expectations. These unique experiments demonstrate not only that TG loading does occur, but that the physics of this phenomenon is understood and must be accounted for in the ITER divertor shaping design.
After presenting the theoretical description of particle deposition in TGs in Section 2, the experimental confirmation by dedicated experiments on COMPASS tokamak is presented in Section 3. The power deposition profiles around TGs calculated by the SPICE2D code for the different field configurations are compared to experimental surface temperature in Section 4. The role of non-ambipolarity together with the results of a dedicated TG biasing experiment on COMPASS, supported by PIC simulations, are shown in Section 5. Finally, the main conclusions are summarized in Section 6.

2. Theory of particle deposition in a toroidal gap

The total magnetic field **B** has two components, one toroidal B_ϕ and one poloidal B_θ. Usually, magnetic flux surfaces are not aligned with the TG gap axis. In ITER divertor, the cassettes holding the vertical targets are tilted [1] with respect to the magnetic flux surfaces with an incidence angle projected onto the plane parallel to the MBs top surface $\theta_{//} = 3.7^o$ at IVT and $\theta_{//} = 5.6^o$ at OVT (see Fig. 1 in [2]). In COMPASS, the pitch angle of the magnetic surfaces, $\mathrm{atan}(B_\theta/B_\phi)$, with respect to the purely toroidally oriented TGs at the experiment location (see Section 3) is similar with $3^o < \mathrm{atan}(B_\theta/B_\phi) < 6^o$, in the range of plasma currents used in the experiments. Therefore, in a purely optical picture, the plasma flowing in the parallel direction impinges preferably only one side of the TG and the deposited heat flux on this side can be described as: $q_{dep} = q_{//,0} \sin(\theta_{//})$, with $q_{//,0}$ the energy flux density parallel to **B**. However,

if the helical trajectories around the magnetic field line of the incoming charged particles are taken into account, this optical picture is not valid anymore. The total particle flux Γ_{tot} is composed of ions and electrons and it can be decomposed around the TG as the sum of the following contributions: (1) a parallel flux Γ_{par} for particles following the OA, (2) a flux due to the Larmor gyro-motion around the field lines Γ_{Larmor} and (3) an **E**×**B** driven flux $\Gamma_{E\times B}$ due to the electric field **E** forming at the MB top surface:

$$\Gamma_{tot} = \Gamma_{par} + \Gamma_{Larmor} + \Gamma_{E\,B} \qquad (2)$$

The electrons can be considered fully magnetized because their Larmor radius $r_{L,e}$ is much smaller than the millimetric gap width (l_{gap}), by roughly 2 orders of magnitude, so their trajectories can be described using the guiding center approximation, i.e., following **B** orientation. Electrons can be thus considered as the main contributors to Γ_{par}.

Considering the ions which can have their Larmor radius $r_{L,i} \sim l_{gap}$ (in ITER ELMy conditions or in COMPASS L-mode conditions), their helical gyro-motion along the field lines must be taken into account and are the main contributors to Γ_{Larmor}. This flux impinges preferentially one side of the TG according to the gyration motion around the field lines (left hand rule).

On the MBs top surface, electric fields pointing towards the surface with strong gradients form. Charges particles that can enter the gap are prone to an **E**×**B** drift that can drive them away from their initial trajectories so that they impinge preferentially the TG side which is located in the direction of that drift and contribute to $\Gamma_{E\times B}$.

By definition both the Larmor flux and the **E**×**B** flux always point in the same direction in the TG since ions with a Larmor flux in the opposite direction do not exist; such orbits are absent from the distribution function because they are scraped-off further upstream. It should be noted that since the electric field always points into the surface, the direction of the **E**×**B** drift, and thus the TG side loaded by $\Gamma_{E\times B}$, only depends on the direction of **B**, which is not the case for the parallel flux, which changes with the direction of B_θ (or of the plasma current I_p). Therefore, it can happen that Γ_{Larmor} and $\Gamma_{E\times B}$ impinge a different side than Γ_{par} for a specific configuration of B_ϕ and B_θ. It has to be noted that both Γ_{Larmor} and $\Gamma_{E\times B}$ always impinge the same side of the TG independently of the orientation (and not the direction) of **B** or independently of the pitch angle. For the sake of clarity, the term *'Larmor/E×B flux'* will be used to refer to those two contributions to Γ_{tot} and will be noted $\Gamma_{Larmor/ExB}$.

By changing the direction of the poloidal and toroidal magnetic fields in the four possible configurations, the theoretical different interactions of a magnetic field line with a TG are examined following the above reasoning and are represented in Fig. 1. The pink arrow, going from left to right, indicates the direction of the incident parallel flow. Within these four different cases, two types of interaction with a TG are observed. The first type of interaction shows that only one side of the TG is loaded by all the different components of the total particle flux as represented in Fig. 1a & 1d. The Larmor/ExB flux points in the same direction as the parallel flux and this is what is predicted to happen at the ITER OVT by ion orbit calculations [2]. The second type of interaction show that both sides of the TG are loaded as represented in Fig. 1b & 1c. The Larmor/ExB flux loads the opposite side of the TG loaded by Γ_{par}, thus by definition the magnetically shadowed side, where the OA predicts no flux. This type of interaction with TG is predicted to happen at the ITER IVT [2]. These predictions are based on 3D ion orbit calculations but such phenomena have never been so far observed experimentally in any tokamak.

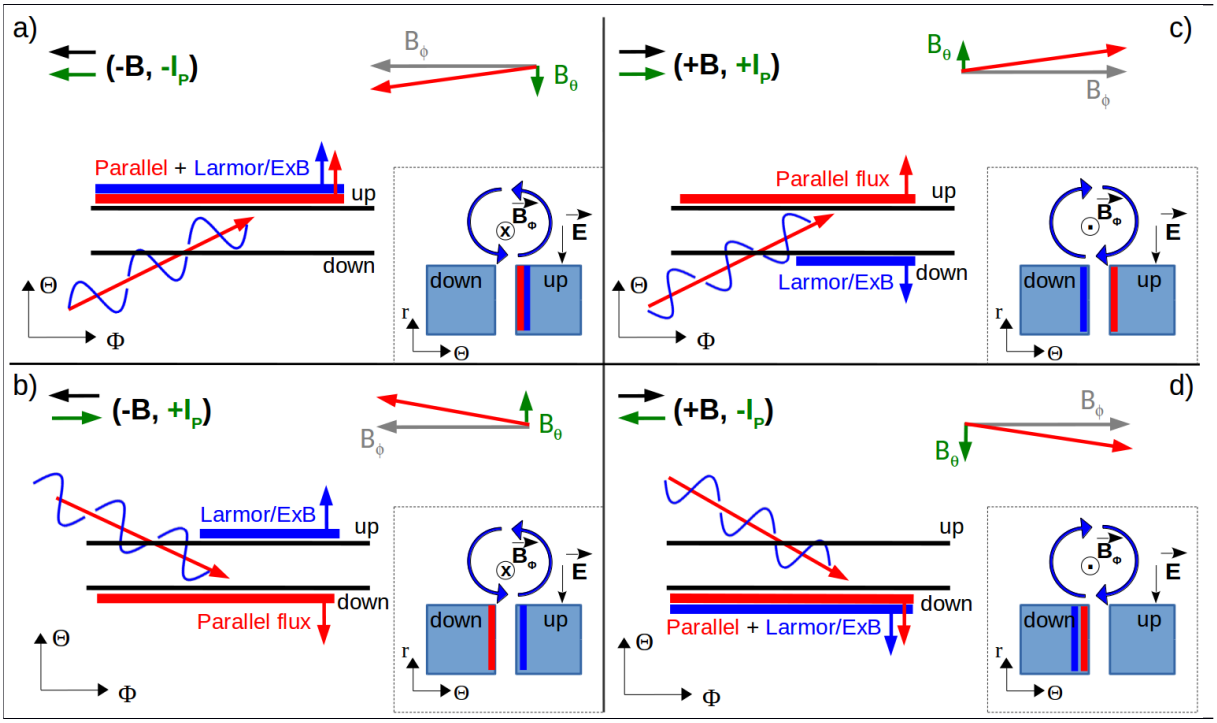

Figure 1: Theoretical representation of the different contributions of the total particle flux (parallel, E×B and Larmor) impinging on a TG in the four possible combinations of B_ϕ and B_θ directions.

3. Experimental confirmation of theoretical predictions

3.1. The COMPASS experimental configuration

A dedicated set of experiments has been performed on the COMPASS tokamak (R = 0.56 m, a = 0.2 m) to thoroughly study TG edge loading and to verify theoretical predictions described in Section 2. A specially designed inner-wall limiter (IWL) is equipped with a 1 mm wide TG cut in a flat surface and is in a direct view of a high resolution infrared camera to monitor the TG edges heating (see Fig. 2). The limiter is made of graphite and has a roof-shape with an apex in the middle protruding above the toroidally neighboring tiles by 8 mm. In the region of interest, where the TG is located, the magnetic field incidence angle projected on the plane perpendicular to the IWL surface and parallel to the toroidal direction is constant toroidally and is $\theta_\perp = 1.5^o$. Because the TG is located on the left side of the apex, when watching the central column from outside as the IR camera views it, the plasma is flowing in the parallel direction only from left to right independently of the **B** direction (see Fig. 2). A poloidally running gap with the same width $l_{gap} = 1$ mm is also present in the middle of the TG at x = -30 mm, recreating the gap crossing in between 4 MBs.

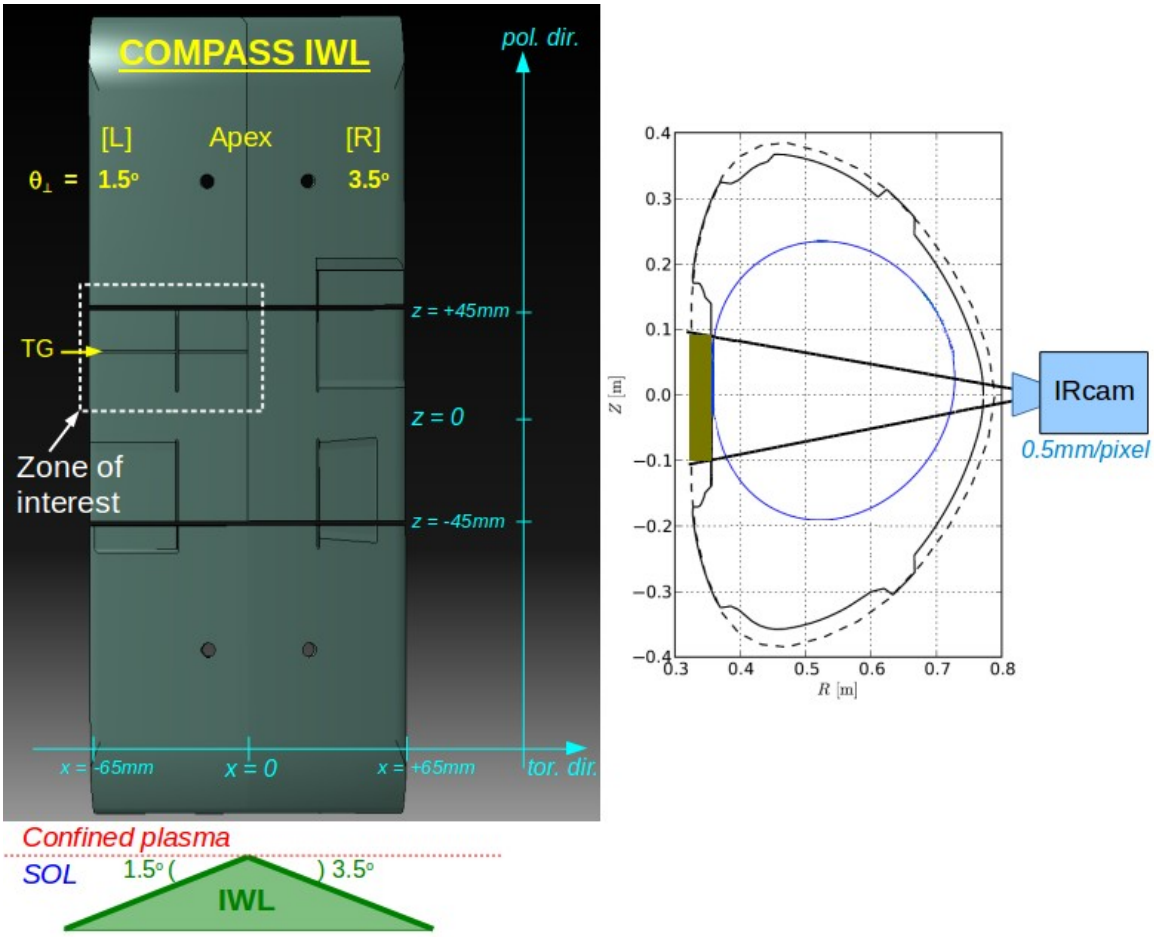

Figure 2: On the left, the schematic views of the COMPASS IWL used in this experimental study with a 1 mm wide TG on the left side of the limiter from the apex, where the magnetic field lines intersect the limiter with $\theta_\perp$ = 1.5°. Below, a scheme of the IWL radial cross-section is drawn. On the right, the scheme of the experimental configuration used in COMPASS experiment with an IR camera is directly viewing the IWL with a high resolution of 0.5 mm/pixel. The slightly elongated plasma contact point is located on the TG.

The experimental configuration is similar to that used in [6-8] to study plasma-wall interactions. The camera used is a mid-IR InSb camera mounted on an outer mid-plane port directly viewing the special IWL. A 50 mm lens was used, yielding a spatial resolution of *r = 0.5 mm/pixel*. Processed data give the surface temperature profiles, $T_{surf,IR}$, in the poloidal direction (coordinate *z* in Fig. 2) across the TG, 10 mm before (x = -40 mm) and 10 mm after the PG (x = -20 mm). Ohmically heated and slightly elongated (κ = 1.1) inner-wall limited deuterium discharges were used with a magnetic field B = 0.9 T, a constant line-averaged density $\acute{n}_e = 3x10^{19}$ m^{-3} and a plasma current I_p = 130 kA, for a total Ohmic input power P_{Ohm} ~ 150 kW. For such discharges, the typical values of the local electron density and temperature from previous measurements with embedded Langmuir probes in a previous IWL [8] are $n_e = 5.10^{18}$ m^{-3} and T_e = 30 eV, respectively. Assuming $T_i = T_e$, this yields a ion Larmor radius $r_{L,i}$ ~ 0.7 mm ~ l_{gap}. This value is comparable to that expected for ELM ions in the ITER divertor. The discharge duration was ~300 ms with a flat top phase of ~150 ms. The plasma column leans on the inner wall with the contact point at a vertical position z = +35 mm on the upper edge of the TG. The standard, forward **B** and I_p direction in COMPASS (clockwise looking from the top), noted (**-B**, **-I$_p$**) by the usual convention and in the rest of this manuscript, yields a pitch angle atan(B_θ/B_ϕ) ~ +6° corresponding to the case a) in Fig. 1 and performed in the COMPASS discharge #11610. In order to reproduce the three other cases, the plasma current direction was changed on a shot-to-shot basis to change the B_θ direction

and therefore the **B** orientation. We remind the reader that since the IWL has an apex located on the right side of the TG region, the only magnetic field lines which intercept the TG come from the left, thus magnetically wetting only one side of the gap. In discharge #11615, the I_p direction was reversed, changing the orientation of the field lines with a pitch angle atan(B_θ/ B_ϕ) ~ -6°, corresponding to the case Fig.1b). By keeping the I_p reversed and now reversing the toroidal field, the pitch angle changes back to atan(B_θ/B_ϕ) ~ +6° but now the configuration corresponds to the case Fig. 1c) where both TG sides should be loaded (discharge #11594). Finally, in the last discharge #11600, the plasma current was changed back to the forward direction to reproduce the configuration Fig. 1d).

3.2. Experimental observations

Poloidal profiles of the surface temperature gradient, $\Delta T_{surf} = T_{surf,IR} - T_{surf,base}$, with $T_{surf,base}$ ~ 80-85°C of the limiter around the gap, across the TG, taken 10 mm before and 10 mm after the PG are plotted in Fig. 3, with each quadrant corresponding to the theoretical configuration of its counterpart in Fig. 1. The poloidal profiles have to be looked at from the right as an observer sitting on the apex and correspond to the schematic insets in Fig. 1.

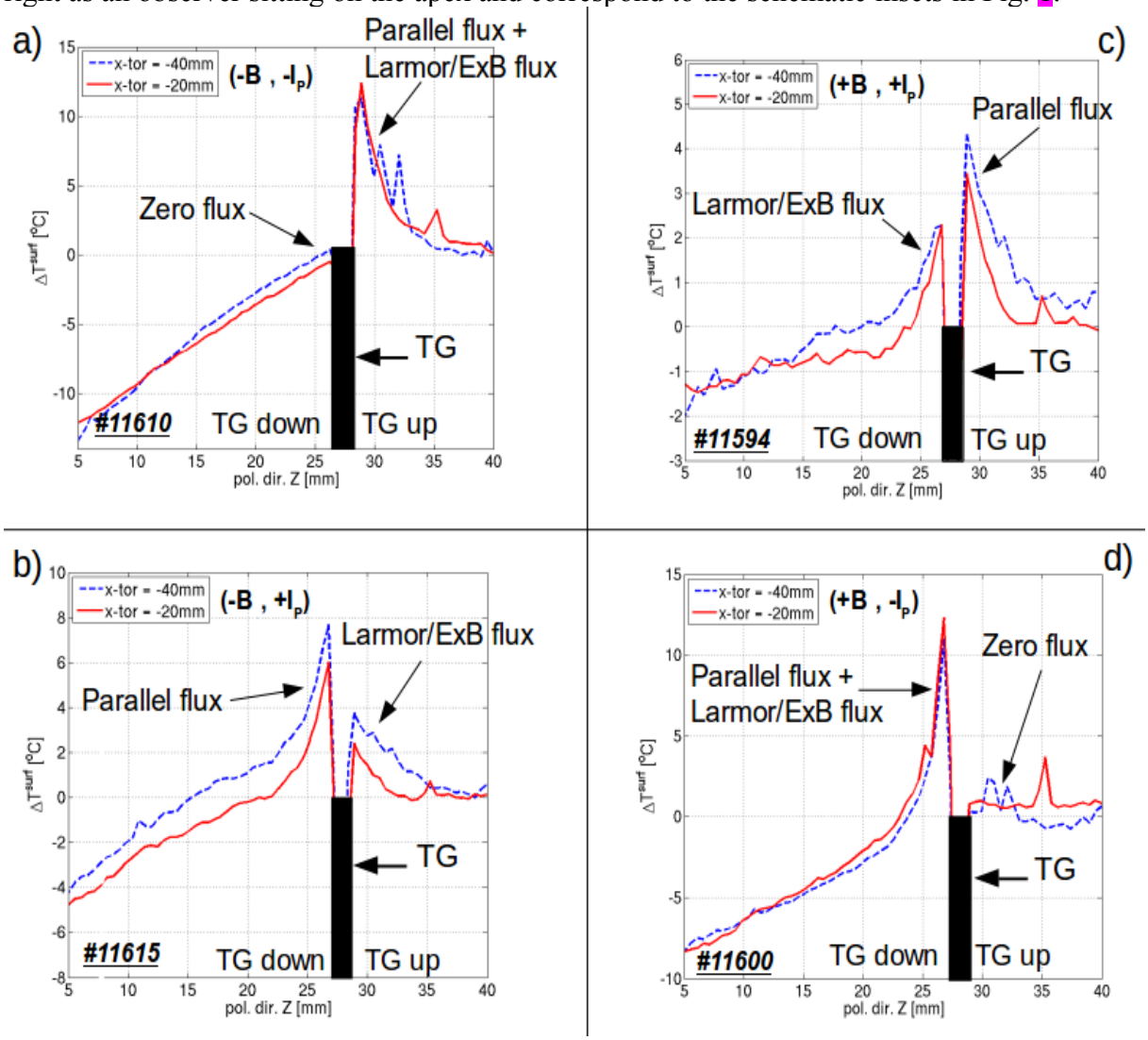

Figure 3: Poloidal profiles of $T_{surf,IR}$ gradient across the TG taken 10 mm before (blue dashed line) and 10 mm after (red line) the PG located in the middle of the TG. Each quadrant corresponds to the same quadrant in

*Fig. 1 showing the theoretical prediction of the different total flux contributions along the TG sides with directions: a) (**-B**, **-I$_P$**), b) (**-B**, **+I$_P$**), c) (**+B**, **+I$_P$**), d) (**+B**, **-I$_P$**).*

The theoretical predictions described in Section 2 have been successfully confirmed experimentally. Fig. 3 shows a good qualitative agreement consistent with the theoretically expected loading.

In the two cases where the theory predicts that both Γ_{par} and $\Gamma_{Larmor/ExB}$ are directed towards the same side of the TG (cases a & d), only one single peak is observed on the $T_{surf,IR}$ profiles on the expected side of the gap. A sharp $T_{surf,IR}$ gradient ($\Delta T_{surf} = 12^oC$) occurring over ~5 mm is observed at the gap corner, which is the signature of local heating of the TG edge. The other side of the TG shows no heating with a zero surface temperature gradient at the gap corner. It can thus be concluded that the magnetically shadowed side of the TG ($z < 27$ mm in Fig. 3a and $z > 28$ mm in Fig. 3d) receives zero flux as predicted by the theory. The slow decrease of $T_{surf,IR}$ away from the bottom side of the gap in all cases for $z < 27$ mm is because the plasma contact point is located slightly above the TG and is representative of the power decay in the SOL.

In the two other cases (b & c) where both sides should be theoretically loaded, two peaks on $T_{surf,IR}$ are observed demonstrating that both gap sides are simultaneously loaded. The side impacted by the parallel flux is always hotter than the Larmor/E×B side, showing twice larger temperature gradient ($\Delta T_{surf,par} \sim 6^oC$) at the corner than on the Larmor/E×B side ($\Delta T_{surf,ExB} \sim 3^oC$), clearly indicating that a stronger effect of the parallel flux. To zero order, the result indicates that the heat load carried by Γ_{par} is ~2 times larger than the one carried by $\Gamma_{Larmor/E\times B}$. Most importantly, these observations represent the first experimental evidence of plasma deposition on the magnetically shadowed side of a TG, where the OA predicts no flux. This effect was predicted for the first time in [2] in the context of a physics study of the required ITER W divertor MB front surface shaping. There it was concluded that ELM-induced loading of TG sides could occur rather readily, even in the case of mitigated ELMs. Until now, however, such TG loading has remained a theoretical concept and has not previously been observed experimentally. The results presented here demonstrate that the effect must now be taken seriously, even if shaping design to avoid TG loading at all locations in the ITER divertor is unlikely to be possible.

4. PIC simulations of plasma deposition in a TG

4.1. Toroidal gap sides heat loading

The deposited particle and heat fluxes profiles along TG sides are calculated using the 2D-3V PIC code SPICE2D [4], which has been previously used in similar studies to calculate plasma deposition profiles inside gaps [5-6,9-10]. The choice of the PIC technique is relevant because it calculates the ion and electron trajectories using three-dimensional velocity vectors in a two-dimensional realistic geometry and in a self-consistent electric field. This allows separating the different contributions from electrons, ions and the ExB drift of the total particle flux. Moreover, the gap size (*1 mm*) is comparable to the ion Larmor radius for the plasma conditions of the experiment (*0.7 mm*). The calculation is made on a square grid having a spatial resolution of one Debye length, which for the conditions of the simulations is $\lambda_D \sim 0.02$ *mm*. SPICE2D simulates the collisionless electrostatic sheath forming around the surface and inside the TG. The magnetic field vector is defined in 3D and assumed constant, which is true to a high approximation over the very short distances (few mm) appropriate for this experiment. Ions are injected into the simulation domain with a velocity distribution function satisfying the Bohm criterion [11]. Electrons are assumed to be Maxwellian. The

case considered here is a fully ionized magnetized plasma with singly charged deuterium ions incident on a completely absorbing, conducting wall. The potential drop in the sheath and magnetic pre-sheath is fixed at $-3kT_e$ with respect to the plasma potential Pot = 0 (thus approximating the case of a floating surface). Due to the symmetry induced by the semi-infinite 2D geometry of the PIC simulation box, the four cases described in Section 2 are reduced to only two cases: (1) only one side of the TG is loaded by all the components of the incoming flux (cases a & d in Fig. 1) and (2) both sides are loaded (cases b & c in Fig. 1). For the purpose of comparison with the experiment, the two configurations a) and b) of Fig. 3 are considered. The low gradients in $T_{surf,IR}$ at the gap edges make the comparison with synthetic temperatures from forward thermal simulations very difficult: a slight variation in the total flux upstream (larger than the experimental resolution) will lead to large errors on the small absolute values of the measured temperatures. Therefore, only the spatial distribution of the heat fluxes calculated by the PIC model will be presented and compared qualitatively with the experimental $T_{surf,IR}$ distribution with the aim of identifying and localizing the three processes at play. For a qualitative comparison, this 1D approximation is good enough since 2D effects should be negligible due to the short time of the experiment (< 300ms). The total power deposition profiles from SPICE2D, noted $q_{PIC,tot}$, as well as the contributions coming from the ions, noted q_i (mainly the Larmor/ExB heat flux, $q_{Larmor/ExB}$), and electrons, noted q_e (mainly the parallel flux q_{par}), are presented in Fig. 4 for both cases of interest and assuming ambipolar conditions. Profiles are normalized to the total flux falling on the IWL top surface far from the perturbation from the gap $q_{\perp,0} = q_{//,0} \sin(\theta_\perp)$. Floating conditions make the fraction of the total energy flux carried by ions dominant with respect to that carried by electrons yielding $q^{PIC,tot} = f*q_i + (1-f)*q_e$, with f = 5/7 [12], as shown in Fig. 4 far from the gap.

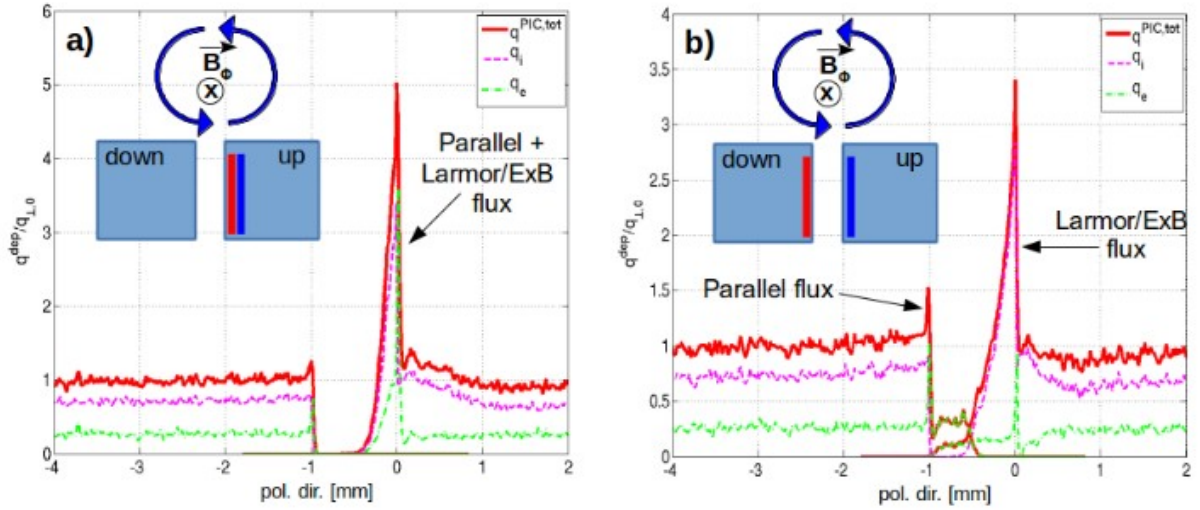

*Figure 4: PIC computed normalized deposited power flux density profiles across a TG with ambipolar conditions corresponding to the two cases of interest in Fig. 4: a) (**-B**, **-I**$_P$) and b) (**-B**, **+I**$_P$).*

The first case shown in Fig. 4a is similar to the experimental finding (Fig. 3a) where all fluxes are deposited exclusively on the magnetically accessible gap side. Both ions and electrons contribute to this total flux, with the latter being totally focused inside the TG and the former, due to their much larger Larmor gyration, spreading their power around the corner onto the top surface. The deposited power inside the gap is made on a distance ~0.5 mm, half the gap width.

The second case shown in Fig. 4b exhibits two peaks similarly to the experimental observations (Fig. 3b), with the peak on the magnetically wetted side of the TG due only to the electron component of q_{par}, and with the peak on the magnetically shadowed side due to

the Larmor/E×B flux, carried mostly by ions. The shadowed side also sees a small contribution from the electrons. This is attributed to those brushing the edge of this side at the corner on their way to the directly wetted side and deeper inside the gap to those deflected by the presence of a negative well in the gap potential as it is illustrated in Fig. 7b. The electron 'streamlines', or contours tangential to average velocity vectors at every grid point of the grid, illustrate the role of strong electric fields inside the gap due to this local negative potential structure. The role of the electric field on the flux distributions is discussed more in details in Section 4.2.

Although the experimental result is qualitatively reproduced, the simulation is unable to reproduce the relative amplitudes of the two peaks. The calculated Larmor/ExB flux at the TG edge is much larger than the projected parallel flux ($q_{Larmor/ExB} > q_{par}\ sin\theta_{//}$ by a factor 2.5), in quantitative disagreement with the experimental observations. As in the case of plasma deposition around a PG [6], the disagreement originates from an overestimate of the ion contribution due to the assumption of ambipolar conditions. A second set of PIC simulations with more realistic non-ambipolar conditions corresponding to $V_{fl} \sim -1kT_e$, which was measured by fixed Langmuir probes in a previous similar COMPASS experiment within 10 mm of the last closed flux surface, confirms this hypothesis. The resulting power deposition profiles for the two cases of interest are presented in Fig. 5, with here the total power mainly carried by the electrons, with the fraction f = 1.2/7 far from the gap.

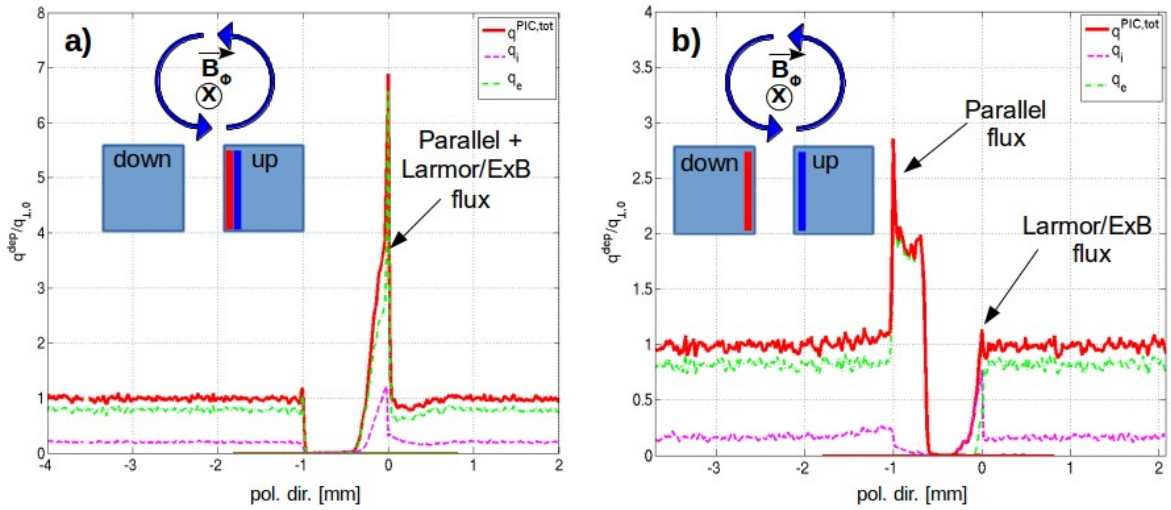

*Figure 5: PIC computed normalized deposited power flux density profiles across a TG assuming here non-ambipolar conditions ($V_{fl} = -1.5kT_e$) corresponding to the two cases in Fig. 4: a) (**-B**, **-I$_P$**) and b) (**-B**, **+I$_P$**).*

For the first case with all components loading the same gap side, the simulation is similar to the previous result with only one peak on the directly wetted side of the TG but now the total energy flux is carried predominantly by electrons (Fig. 5a). Due to a smaller potential drop in the electrostatic sheath, the peak amplitude is 40% higher than in the ambipolar case. Changes are more drastic in the second where the peak amplitude asymmetry observed in Fig. 4b has now switched sides and is in better qualitative agreement with experiment (Fig. 5b). Electrons continue to follow the OA, but with higher energy, so that the parallel flux now makes a larger contribution to q_{tot} leading to increased loading on the magnetically wetted side. Thanks to their gyro-motion, the ions are still able to impact on the shadowed side of the TG, where the OA predicts no accessibility, but now with a smaller contribution. The deposition of electrons on the magnetically shadowed side of the gap is explained similarly to the ambipolar case with a negative well in the electric potential inside the gap that deflects some electrons.

4.2. Role of electric fields in the TG plasma deposition

In order to investigate the role of electric fields more in detail, ballistic simulations have been performed by SPICE2D, i.e. PIC simulations where the electric field was forced to zero. Fig. 6 shows a direct comparison of ion power deposition profiles along the TG sides with ambipolar conditions with electric fields (PIC) and without (ballistic) for the two cases a) and b) of Fig. 3. Profiles have been normalized in each case to the ion heat flux falling on the IWL top surface far from the gap.
In the case b) of a 2-sided TG deposition, the presence of electric field reduces the top surface loading at the magnetically wetted corner downstream and enhances heat loading at the magnetically shadowed side inside the TG (Fig. 6b). The latter effect is due to the presence of a negative potential well in the gap that accelerates ions. This is illustrated in Fig. 7c & 7d that show the ion streamlines for the ballistic and PIC simulations of Fig. 6b.

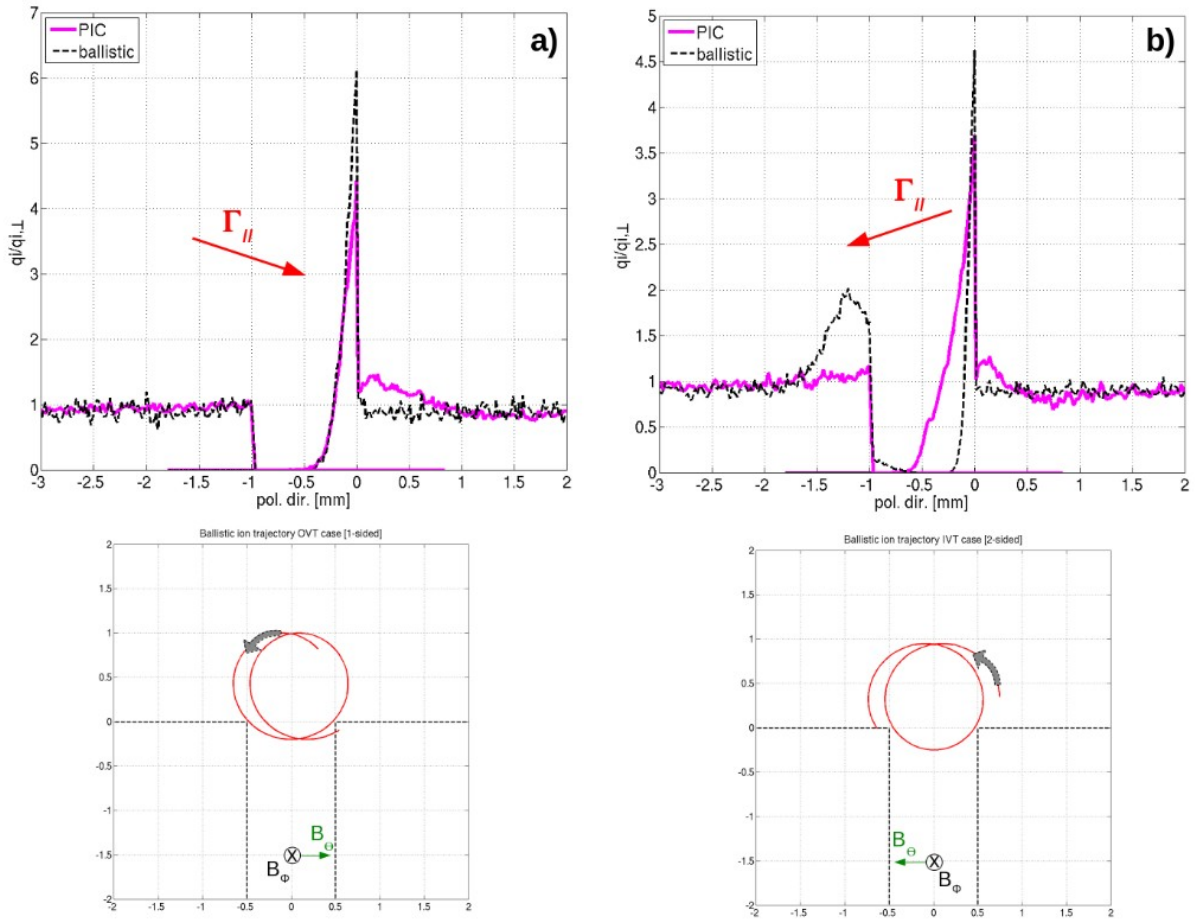

*Figure 6: PIC and ballistic ion power deposition profiles inside a TG normalized to the power flux falling on the IWL top surface far from the gap with ambipolar conditions for the case b) of Fig. 4 (**-B**, **+I$_P$**) corresponding to the two-sided TG heat loading. Below each figure, a scheme of an incoming ion ballistic trajectory to illustrate the extra ion deposition on the magnetically wetted TG side in both cases.*

It is seen that ions can penetrate deeper into the gap in the presence of electric fields. The electric potential, which is plotted in the background of Fig. 7d, exhibits in the gap a more negative potential (Pot ~ -4Te) than the floating potential and can deflect incoming ions from their ballistic trajectories to push them deep into the gap. This potential well is explained by most ions not entering the gap, as seen on the ballistic streamlines (Fig. 7c), on the contrary to electrons which can enter the gap following an optical path (Fig. 7a) and thus creating a negative difference of charge. This is the opposite to what happens in PGs where ions can jump into the gap thanks to their Larmor gyration, whilst electrons cannot, thus creating a

positive structure in the gap potential capable of reaching values higher than the plasma potential Pot = 0 under certain conditions [5,13]. The downstream extra heat flux observed in the ballistic case in Fig. 6b comes from ions that manage to make a full rotation within the gap before striking the downstream top surface, as illustrated in the scheme below the graph. This is possible because the ion Larmor radius (0.7 mm) in the COMPASS experiment conditions is smaller than the gap width (1 mm). This extra heat flux is not present when the electric field is on because when an ion enters the gap it does not go out but is accelerated deeper into the gap by the negative potential well towards the upstream, magnetically shadowed Larmor/ExB side. The same process occurs for electrons but now the potential well reflects the incoming electrons towards the magnetically shadowed side. This explains the electron heat load contribution on the magnetically shadowed side observed in Fig. 4b. This mechanism is illustrated by the streamlines in Fig. 7b. It can be noted that for ITER ELMy conditions, no discrepancy is observed between PIC and ballistic simulations on both sides because there is a positive potential structure on this side of the gap that prevents incoming ions to reach the gap side [14]. Moreover, for an ion temperature of 5 keV in the ITER 15 MA/5.3 T scenario, the resulting ion Larmor radius is r_{Li} = 2 mm [2] and is 4 times larger than the gap width in between MBs (l_{gap} = 0.5 mm). Therefore, ions which can make a single rotation in the gap before reaching the downstream corner are absent from the distribution and there is no extra contribution in the heat flux, as in the COMPASS case.

In the case a) of a 1-sided TG deposition (Fig. 6a), the two profiles are very similar indicating that the role of electric fields is marginal. In the ballistic case, the same mechanism as in the 2-sided deposition is responsible for the slightly larger gap side loading. Incoming ions with a Larmor radius smaller than the gap width can make a full gyration inside the gap before impinging on the TG side, as illustrated in the scheme in Fig. 6a,

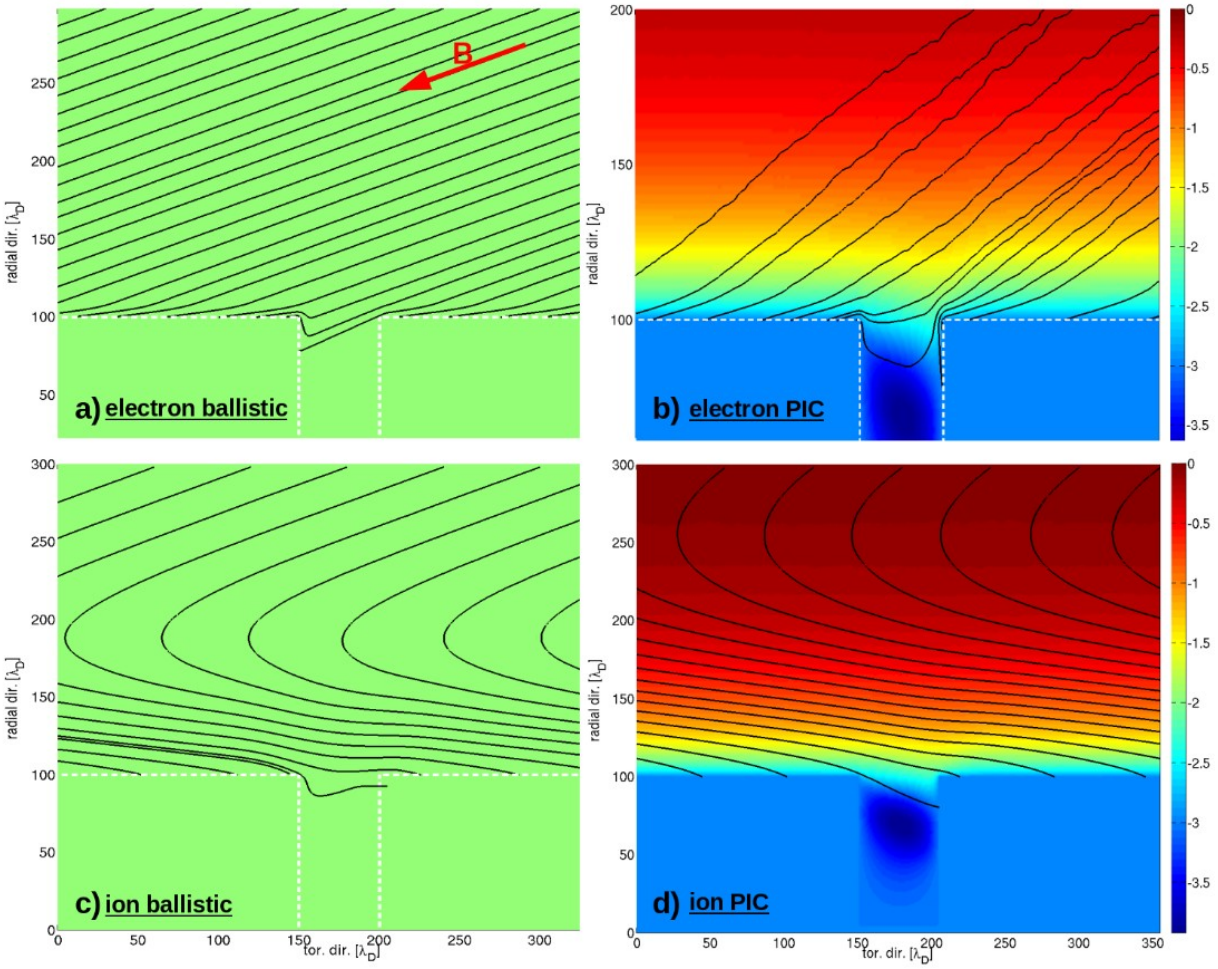

*Figure 7: Computed electron streamlines for the ballistic case (a) and PIC with ambipolar conditions (b) and ion streamlines for the ballistic case (c) and PIC with ambipolar conditions (d) around the COMPASS TG for case b) of Fig. 4 (**-B**, **+I_P**) corresponding to the two-sided TG heat loading. In the background, the electric potential decays from the plasma potential (zero volt) to the floating potential (-3kTe) at the IWL surface and reaching even more negative values ~-4Te in the gap.*

At the top surface, incoming ions are gradually scraped-off from the plasma as they arrive closer to the IWL top surface as a result of their Larmor gyro-motion and the grazing incidence angle of the field lines. This creates a local decrease of ion density and gives rise to an apparent velocity component pointing toward the surface, simply because ions moving out the surface are missing in the distribution. It is illustrated in Fig. 7c by the change of direction of their streamlines above the surface in the magnetic presheath. In the presence of electric fields, this effect is enhanced by an ExB drift in the same direction (B_ϕ is pointing towards the page in Fig. 7) but this effect is reduced in the Debye sheath close to the top surface because of a polarization drift. The polarization drift is the direct consequence of ions passing through the sheath and experiencing a temporally evolving local electric field in their frame of reference [5].

5. Role of non-ambipolarity: the TG biasing experiment

In order to investigate experimentally the role of non-ambipolarity described in Section 4.1., a recent dedicated experiment has been performed in COMPASS. A new IWL with the same geometry as the previous one has been built with now two embedded graphite blocks where TGs are cut. The blocks lie on boron nitride beds to insure electrical insulation and are connected to a power supply allowing biasing of the TGs. The insulated TGs are located from

each side of the apex with a constant incidence angle $\theta_{\perp} = 2.5^{o}$ for both wings. The block on the left side present only one TG, whilst the block on the right presents both a TG and a PG (Fig. 8c). The results presented here are for the right block including the gap crossing but identical results are present on the left block. Similar experimental configuration and plasma conditions as described in Section 3.1., where **B** and Ip directions were changed to reach the 4 possible configurations of field lines interactions, were used. Different voltage waveforms were applied (square or triangular) to sweep the biasing voltage from zero volt (grounded) to -180 V (ambipolar conditions), in order to force conditions to go from an electron dominated regime as in the original experiment (Fig. 3) to an ion dominated regime (Fig. 4). The values of -180V has been chosen to be at least at -3Te below the floating potential estimated at V_{fl} = -30 to -50 V from previous similar experiments. In total, 12 discharges were performed and all results are consistent with the ones presented in the paragraph below, where only the most interesting theoretical case b) of Fig. 1 will be presented for the sake of concision of this paper, corresponding to the two-sided TG heat loading case.

In the discharge of interest with forward **B** and Ip, the pitch angle is $\text{atan}(B_{\theta}/B_{\phi}) \sim +6^{o}$ and since the observed TG is now located on the right side of the apex, the parallel flux comes only from the right and impinges the lower side of the TG for the same interaction as described in Fig. 1b with the Larmor/ExB side being the TG upper side. The applied voltage has a triangular shape with a sweeping period of 120 ms (Fig. 8a), long enough to allow thermal response of the graphite block. Similar temperature gradients as defined in Section 3.2. are presented in Fig. 8b along the line of view located downstream the PG and indicated on the IR camera image in Fig. 8c.

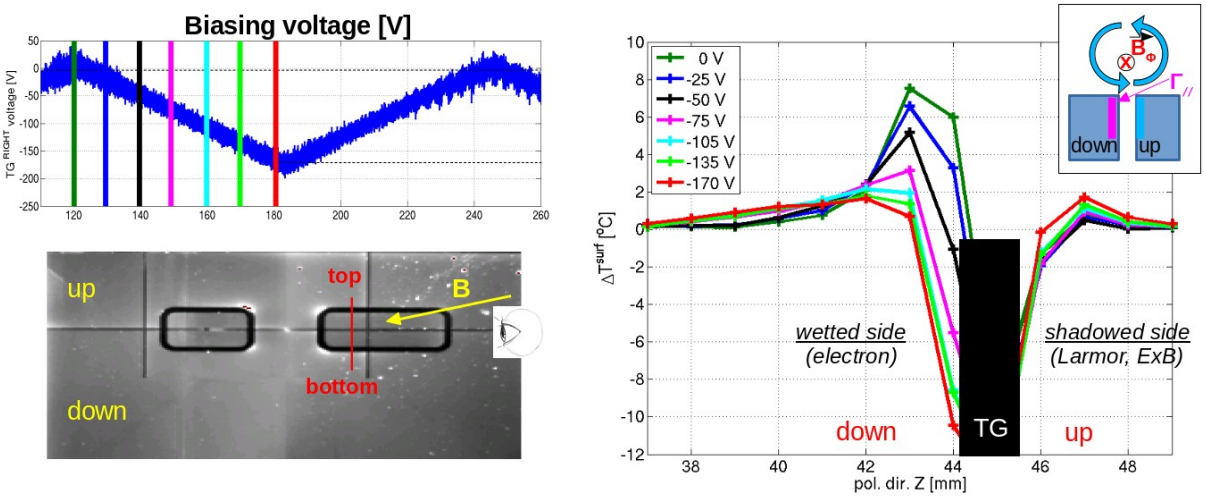

Figure 8: a) Applied voltage waveform from 0 to -180 V with a period of 120 ms, b) corresponding $T_{surf,IR}$ gradients around the TG for different voltages and 3) snapshot of the IR camera with the line of view of $T_{surf,IR}$ profiles indicated in red and the pitch angle indicated by the yellow arrow.

The $T_{surf,IR}$ distribution around the TG when zero volt is applied corresponds to the grounded case as presented in Fig. 3. When the applied voltage is gradually decreased to -180 V, the temperature gradient at the downstream, directly magnetically wetted side gradually decreases from $\Delta T_{surf,IR} = 8^{o}C$ to $\Delta T_{surf,IR} = 2^{o}C$. This is the direct consequence of the strong reduction of the electron contribution, or q_{par}, in ambipolar conditions. On the magnetically shadowed, Larmor/ExB side the effect is opposite with an increase of $\Delta T_{surf,IR}$ as expected by the theory with the increase of $q_{Larmor/ExB}$ with ambipolar conditions. The increase is however not very significant ~$1.5^{o}C$ going from $\Delta T_{surf,IR} = 0.5^{o}C$ (non-ambipolar) to $\Delta T_{surf,IR} = 2^{o}C$ (ambipolar). It has to be noted that due to the combination of the short duration and low power COMPASS discharges and no leading edge, the TG edge heating is not significant but such effect on both sides is observed systematically in all investigated discharges. The change in the

asymmetrical TG heat loading from one side to the other predicted by PIC simulations occurring when ambipolarity is broken has been recreated experimentally. It demonstrates the role of local non-ambipolarity in TG edge heating and that this must be taken into account in predictive calculations.

6. Summary and conclusion

This paper describes the physics of toroidal gap heat loading when the ion Larmor radius is of the same size or larger than the gap width. The total flux density impinging the gap sides comprises 1) a parallel to magnetic field component mainly carried by electrons, 2) an ion contribution resulting from the large Larmor gyro-motion and 3) an E×B drift due to the strong sheath electric fields. Finite Larmor radius effects dominate ion deposition with the poloidal component of the ion flux striking the surface always in the diamagnetic drift direction. Depending on the directions of the poloidal and toroidal magnetic fields, the different heat flux components will load either one same side (ITER OVT case) or both sides (ITER IVT case) of the gap, thus in the latter case loading the magnetically shadowed side where the optical approximation predicts no flux. The theoretically predicted toroidal gap edge loading on the magnetically shadowed side was confirmed experimentally for the first time on the COMPASS tokamak proving that this effect is real. Toroidal gap edge heating has been unequivocally observed by measuring surface temperature increases across gap by high resolution IR camera in the four possible field line interactions with a toroidal gap. Experimental results are qualitatively well reproduced by 2D-3V PIC simulations. However, the simulations must invoke non-ambipolarity in the gap vicinity, consistent with data obtained from tile embedded Langmuir probes under similar conditions, to fully explain the observed relative peak loading amplitudes on each side of the gap across all total magnetic field directions. A strong experimental confirmation of the proposed local non-ambipolarity was achieved in a recent experiment by biasing the TG negatively with respect to the surrounding limiter. In the case of the two-sided deposition and depending on the bias voltage, the heat load is observed to switch sides, following theoretical expectations. The role of the sheath electric field is assessed by comparing PIC and ballistic simulations. In the case of a 1-sided deposition on the directly wetted side, the profiles are very similar indicating the role of electric fields is marginal. In the case of a 2-sided deposition, the presence of electric fields reduces the top surface loading at the downstream corner and enhances heat loading at the magnetically shadowed side inside the gap. This is caused by the presence of a negative potential well that accelerates ions that enter the gap, instead of allowing them to make a full revolution before impinging the top surface downstream corner because of a Larmor radius smaller than the gap width. However, it can be noted that for ITER ELMy conditions, no discrepancy is observed between PIC and ballistic simulations because of a positive potential structure in the gap because of ion Larmor radii much larger than the gap width. The results from this unique set of experiments and PIC simulations demonstrate not only that TG loading does occur but that the physics of this phenomenon is understood and must be accounted for in the ITER divertor shaping design.

Acknowledgement

This work was supported by the project Czech Science Foundation GA16-14228S and has been co-funded by the MEYS projects 8D15001 and LM2015045. This work has been carried out within the framework of the EUROfusion Consortium (WP PFC) and has received funding from the Euratom research and training programme 2014-2018 under grant agreement No 633053. The views and opinions expressed herein do not necessarily reflect those of the European Commission or of the ITER Organization.

References

[1] S Carpentier-Chouchana et al., Phys. Scr. **T159** (2014) 014002

[2] J P Gunn et al., Nucl. Fusion **57** (2017) 046025 (35pp)

[3] J P Gunn et al., Nuclear Materials and Energy **12** (2017) 75-83

[4] R Dejarnac and J P Gunn, J. of Nucl. Mater. **363-365** (2007) 560-564

[5] M Komm et al., Nucl. Fusion **57** (2017) 1260470 (12pp)

[6] R Dejarnac et al., Nucl. Fusion **58** (2018) 066003 (14pp)

[7] J Horacek et al., J. of Nucl. Mater. **463** (2015) 385-388

[8] R Dejarnac et al., J. of Nucl. Mater. **463** (2015) 381-384

[9] R Dejarnac et al., J. Nucl. Mater. **390-391** (2009) 818-821

[10] R Dejarnac et al., IEEE Transactions on Plasma Science, vol.**38**, no.4 (2010) 1042-1046

[11] J P Gunn, J. of Nucl. Mater. **337-339** (2005) 310-314

[12] P C Stangeby, '*The plasma boundary of magnetic fusion devices'*, IoP Publishing Ltd

[13] M Komm et al., Plasma Phys. Control. Fusion **53** (2011) 115004 (11pp)

[14] R Dejarnac, M Komm and J P Gunn, ITER contracts, private communication.